

# Morphology of the Nuclear Disk in M87

Z.I. Tsvetanov<sup>1</sup>, M.G. Allen<sup>1,2</sup>, H.C. Ford<sup>1,3</sup>, and R.J. Harms<sup>4</sup>

<sup>1</sup> Johns Hopkins University, Baltimore, MD 21218, USA

<sup>2</sup> Mount Stromlo and Siding Spring Observatories, ACT 2611, Australia

<sup>3</sup> Space Telescope Science Institute, Baltimore, MD 21218, USA

<sup>4</sup> RJH Scientific, 5904 Richmond Highway, Alexandria, VA 22303, USA

**Abstract.** A deep, fully sampled diffraction limited (FWHM  $\sim 70$  mas) narrow-band image of the central region in M87 was obtained with the Wide Field and Planetary Camera 2 of the *Hubble Space Telescope* using the dithering technique. The H $\alpha$ + [N II] continuum subtracted image reveals a wealth of details in the gaseous disk structure described earlier by Ford et al. (1994). The disk morphology is dominated by a well defined three-arm spiral pattern. In addition, the major spiral arms contain a large number of small “arclets” covering a range of sizes ( $0''.1-0''.3 = 10-30$  pc). The overall surface brightness profile inside a radius  $\sim 1''.5$  (100 pc) is well represented by a power-law  $I(\mu) \sim \mu^{-1.75}$ , but when the central  $\sim 40$  pc are excluded it can be equally well fit by an exponential disk. The major axis position angle remains constant at about  $\text{PA}_{\text{disk}} \sim 6^\circ$  for the innermost  $\sim 1''$ , implying the disk is oriented nearly perpendicular to the synchrotron jet ( $\text{PA}_{\text{jet}} \sim 291^\circ$ ). At larger radial distances the isophotes twist, reflecting the gas distribution in the filaments connecting to the disk outskirts. The ellipticity within the same radial range is  $e = 0.2 - 0.4$ , which implies an inclination angle of  $i \sim 35^\circ$ . The sense of rotation combined with the dust obscuration pattern indicate that the spiral arms are trailing.

## 1 Introduction

The disk of ionized gas in the nucleus of M87 is currently the best example of a family of similar small ( $r \sim 100$  pc) gaseous disks found to be common in the centers of elliptical galaxies with active nuclei (for a review see Ford et al. 1998). Several *HST* kinematical studies have shown that in M87 the gas is in Keplerian rotation, orbiting a massive black hole with a mass  $M_{\text{BH}} \sim 2 - 3 \times 10^9 M_\odot$  (Harms et al. 1994; hereafter H94, Ford et al. 1996a,b; and Macchetto et al. 1997, hereafter M97). The few other galaxies studied kinematically so far (NGC 4261 – Ferrarese et al. 1996, NGC 6521 – Ferrarese et al. 1998, NGC 4374 – Bower et al. 1998) have further shown that nuclear gaseous disks offer an excellent tool for measuring the central black hole mass.

Recent studies have revealed other important characteristics of the nuclear disk in M87. Its apparent minor axis (F96, M97) is closely aligned with the synchrotron jet ( $\Delta\theta \sim 10^\circ - 15^\circ$ ) suggesting a causal relationship between the disk and the jet. The system of filaments in the center of M87 (Sparks, Ford & Kinney 1993; SFK) may also be causally connected to the disk. For example, the filaments extending  $\sim 17''$  (1200 pc) to the NW at  $\text{PA} \sim 315^\circ$  are blue shifted

with respect to systemic velocity and show dust absorption implying they are on the near side of M87 as is the jet. These two findings led SFK to conclude that these filaments are streamers of gas flowing away from the center of M87 rather than falling into it. The images in F94 (see also Ford & Tsvetanov, this volume, FT98) show an apparent connection between at least some of the larger scale filaments and the ionized nuclear disk.

Direct spectroscopic evidence for an outflow was found recently. Several UV and optical absorption lines from neutral and very mildly ionized gas were measured in the FOS spectrum of the nucleus (Tsvetanov et al. 1998; T98). These lines are broad (FWHM  $\sim 400 \text{ km s}^{-1}$ ) and blue shifted by  $\sim 150 \text{ km s}^{-1}$  with respect to M87's systemic velocity implying both an outflow and turbulence. In addition, non-circular velocity components – both blue and red shifted – were found at several locations in the disk (F96, FT98), and observed emission lines are much broader than the expected broadening due to the Keplerian motion across the FOS aperture. All these properties are best understood if a bi-directional wind from the disk were present. This wind may be an important mechanism for removing angular momentum from the disk to allow accretion through the disk onto the central black hole.

Whatever the physical conditions in the disk it is important to map its morphology in detail. The first *HST* images (F94) have hinted that a spiral pattern could be present, but the signal-to-noise was too low for a definitive conclusion. In this paper we present deep, fully sampled diffraction limited narrow band images of the nuclear region in M87. We use these images to characterize the ellipticity, brightness distribution, and morphology of the disk. In this paper we adopt a distance to M87 of 15 Mpc, corresponding to a scale of  $1'' = 73 \text{ pc}$ .

## 2 Observations

M87 was imaged through the WFPC2 narrow-band filter F658N (central wavelength/effective width =  $6590/28 \text{ \AA}$ ) which isolates the  $\text{H}\alpha + [\text{N II}]$  emission line complex at the systemic redshift. The nucleus was placed near the center of the planetary camera (PC) and the *HST* roll angle was  $307^\circ$ , orienting the M87 synchrotron jet roughly along the diagonal of the PC field of view.

The PC has a scale of  $45.54 \text{ mas pixel}^{-1}$  (Holtzman et al. 1995) and under-samples the *HST* diffraction limited PSF at all wavelengths shorter of  $\sim 1\mu$ . To achieve full sampling we took images at four adjacent positions, offsetting the telescope by 5.5 PC pixels between each images – the so called dithering technique. The pattern used is illustrated in Fig. 1. At each of the four subpixel positions we took 3 images for cosmic ray rejection and cleaning of permanent defects. We re-calibrated the images using the best recommended calibration files.

To build a fully sampled image we used the variable-pixel linear reconstruction algorithm (informally known as “drizzling”) developed originally for the Hubble Deep Field (Fruchter & Hook 1997). The relative offsets of individual images were estimated from the positions of good signal-to-noise objects in the

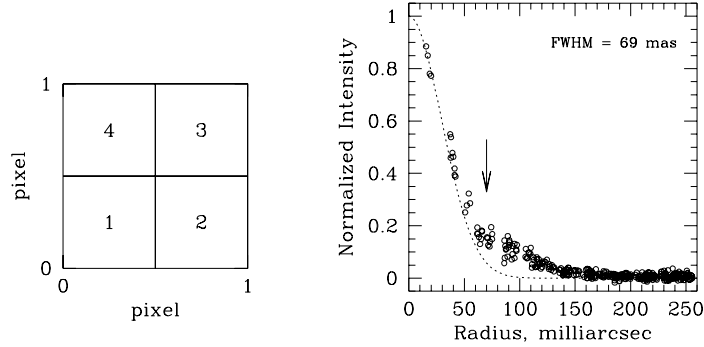


**Fig. 1.** *Left* panel illustrates the dithering pattern. Three images were taken at each of the positions numbered 1 to 4. The telescope offset was 5.5 PC1 pixels between positions. The *right* panel shows the radial profile of an unsaturated star  $\sim 6''$  south of nucleus. The overplotted Gaussian has a FWHM equal to the *HST* diffraction limit at the wavelength of observation (6580 Å). The first Airy ring is marked by the arrow.

field and also through a 2-D cross correlation. Both techniques yielded similar results. No significant offsets were found for the three frames taken at each one of the subpixel positions. These were combined to remove the cosmic ray events. The four combined frames were then combined on an output grid of 25 mas  $\text{pixel}^{-1}$  using the drizzling algorithm. The 25 mas pixel size is a good match for the  $\sim 70$  mas *HST* diffraction limit at  $\text{H}\alpha$ . This is illustrated by the radial profile of a star in the field shown in Fig. 1 where the first Airy ring is clearly seen.

Because of serious observing time restrictions, and also because the underlying galaxy profile is known to be smooth, no continuum images were obtained simultaneously with the on-line ones. To create a suitable off-band image for continuum subtraction we used a number of M87 images from the *HST* public archive. These include a series of F814W images taken on November 11, 1995, which have small relative offsets that allow us to build a fully sampled image using the same drizzling technique. The offset pattern is not ideal (as in the case of F658N), but this is less critical because of the smooth shape of the continuum light distribution.

To form an image suitable for continuum subtraction at the wavelength of  $\text{H}\alpha$  we used a  $(V - I)$  color image to correct the F814W image for color effects, which are particularly important at the positions of the dust bands. Finally, the continuum subtracted  $\text{H}\alpha + [\text{N II}]$  image was flux calibrated using the estimated system throughput at the redshifted position of  $\text{H}\alpha$  and the averaged measured  $[\text{N II}]/\text{H}\alpha$  line ratio.

### 3 Disk morphology

The central  $1'' - 2''$  of the continuum subtracted  $H\alpha + [N II]$  image (Fig. 2, left panel) is dominated by a clockwise winding 3-arm spiral pattern superposed on an underlying disk-like morphology. At larger radial distances the gaseous structure is less well organized, asymmetric, and gradually transition into the larger scale  $H\alpha$  filaments. Several of these filaments can be traced to connect to the disk but none appears to go directly into the nucleus.

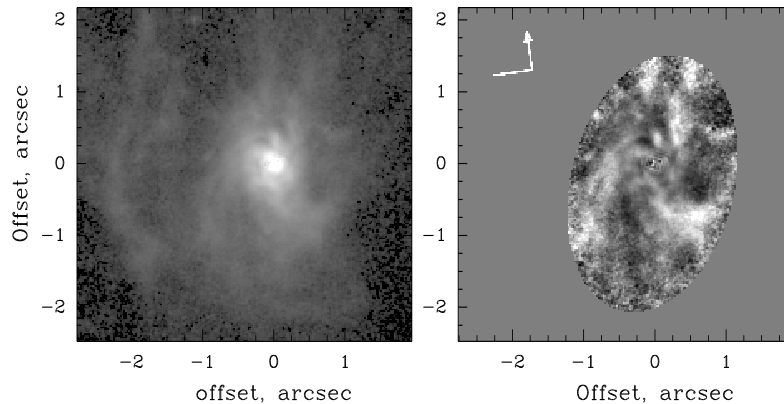


**Fig. 2.** The  $H\alpha + [N II]$  continuum subtracted image is shown in the *left* panel. The gray scale saturates the central few pixels, which are uncertain due to the imperfect color matching and variability of the central point source. The *right* panel shows the ratio of the observed structure to the smooth disk model, as discussed in the text. The image is stretched linearly between  $\pm 70\%$  relative to the model.

To estimate the parameters describing the surface brightness profile, ellipticity and orientation, we have performed an elliptical isophote analysis. We started by setting all parameters free, and gradually introduced constraints such as fixed center position, major axis position angle and/or ellipticity, in an attempt to explore the robustness of the solution. To our satisfaction the values for all major parameters of the fit remained stable regardless of the constraints used.

Fig. 3 shows the surface brightness radial profile, major axis position angle, and ellipticity as a function of radial distance. Outside  $r \sim 0''.5$  (40 pc), the surface brightness profile is well described by an exponential disk with an effective radius of 45 pc. There is, however, a significant excess of light in the central  $0''.5$ , and a single power law  $I_{pl} \sim (r/50)^{-1.75}$  is a better representation of the overall profile. In the region 20–90 pc, the orientation of the major axis remains roughly constant at  $PA_{maj} \sim 6^\circ$ . At the same time the ellipticity increases smoothly from 0.2 to 0.4. The constancy of  $PA_{maj}$  is usually interpreted as a signature of a disk, while the ellipticity could be influenced by the spiral arms or there could be a warp. The central few points are less reliable because of possible color mismatch

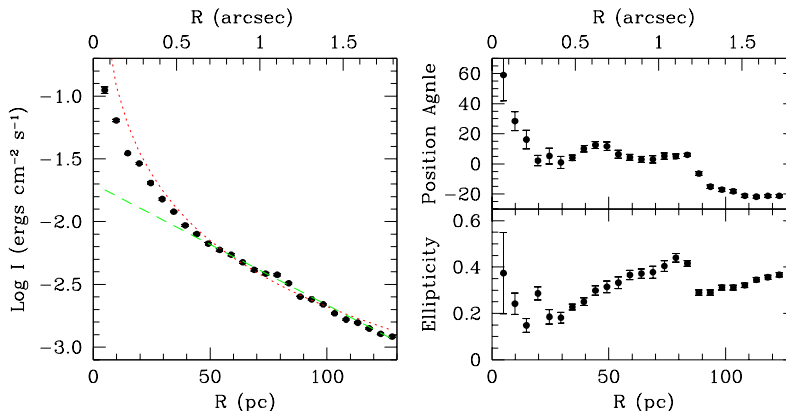


**Fig. 3.** *Left:* The surface brightness profile of the M87 nuclear gaseous disk. The short dashed line is a power law  $I_{pl} \sim (r/50)^{-1.75}$ , and the long dashed line is an exponential disk with  $I_{disk} \sim \exp(-r/45)$ , where  $r$  is in pc. *Right:* The radial dependence of the major axis position angle ( $PA_{maj}$ ) and ellipticity ( $e$ ).

of the on- and off-band images and the variability of the nuclear point source (T98).

The kinematic studies (F96, M97) have shown that the north part of the disk is receding and the south part is approaching and the estimated inclination is consistent with the one inferred from isophote analysis. The obscuration patches on the SE side (F94) indicate that the SE side is closer to us. Combining all this information indicates that the spiral arms are trailing.

This work is supported by NASA grant NAG-1640 to the HST FOS team.

## References

- Biretta, J. A., Stern, C. P., & Harris, D. E. 1991, *AJ*, 101, 1632 (BSH91)  
 Bower, G. et al. 1998, *ApJ*, 492, L111  
 Ferrarese, L., Ford, H. C., & Jaffe, W. 1996, *ApJ*, 470, 444  
 Ferrarese, L., Ford, H. C., & Jaffe, W. 1998, *ApJ*, in press  
 Ford, H. C. et al. 1994, *ApJ*, 435, L27 (F94)  
 Ford, H. C. et al. 1996, in *Nobel Symp. 98, Barred Galaxies and Circumnuclear Activity*, ed. A. Sandqvist & P. Lindblad (Heidelberg: Springer-Verlag), 293  
 Ford, H. C. et al. 1998, in *IAU Symp. 184, The Central Regions in the Galaxy and Galaxies*, in press  
 Fruchter, A. S., & Hook, R. 1997, <http://www.stsci.edu/~fruchter/dither>  
 Harms, R. J. et al. 1994, *ApJ*, 435, L35 (H94)  
 Holtzman, J. A. et al. 1995, *PASP*, 107, 156  
 Macchetto, F. et al. 1997, *ApJ*, 435, L35 (M97)  
 Sparks, W. B., Ford, H. C., & Kinney, A. 1993, *ApJ*, 413, 531 (SFK)  
 Tsvetanov, Z. I. et al. 1998, *ApJ*, 493, L83 (T98)